Accurate and efficient evolution of nonlinear Schrödinger equations

Roi Baer*
Department of Physical Chemistry and The Lise Meitner Minerva-Center for Quantum Chemistry, The Hebrew University of Jerusalem, Jerusalem 91904, Israel
(Received 25 April 2000; published 13 November 2000)

A numerical method is given for affecting nonlinear Schrödinger evolution on an initial wave function, applicable to a wide range of problems, such as time-dependent Hartree, Hartree-Fock, density-functional, and Gross-Pitaevskii theories. The method samples the evolving wave function at Chebyshev quadrature points of a given time interval. This achieves an optimal degree of representation. At these sampling points, an implicit equation, representing an integral Schrödinger equation, is given for the sampled wave function. Principles and application details are described, and several examples and demonstrations of the method and its numerical evaluation on the Gross-Pitaevskii equation for a Bose-Einstein condensate are shown.

PACS number(s): 03.75.Fi, 31.15.−p, 42.65.−k

I. INTRODUCTION

Nonlinear Hamiltonians and Schrödinger equations often arise when many-particle quantum dynamics are reduced to effective one-particle quantum motion. Typical examples are the time-dependent Hartree-Fock [1], Hartree [2], and density-functional theories [3], as well as the Gross-Pitaevskii [4] equation for the dynamics of a Bose-Einstein condensate (BEC). Typically, an initial value propagation problem [with $\psi(\mathbf{r},t=0)=\phi(\mathbf{r})$] is encountered,

$$i\hbar\frac{\partial\psi}{\partial t}=-\frac{\hbar^2}{2\mu}\nabla^2\psi+V(\mathbf{r})\psi+W(\mathbf{r},t,\{\psi(t)\})\psi, \qquad (1)$$

where $\psi(t)=\psi(\mathbf{r},t)$ is the time-dependent wave function for an effective particle in an n-dimensional spatial vector $\mathbf{r}$ (typically, $n=1$, 2, or 3); $\hbar=h/2\pi$, where h is Planck's constant; and μ is the effective particle mass. The linear operator $V(\mathbf{r})$ represents an external potential usually a trap for confining the particles, while $W(\{\psi(t)\},\mathbf{r},t)$ is the term, which includes the nonlinear potential, resulting from the original particle-particle interactions, and any explicit time-dependent field applied on the system.

A numerical scheme for solving the nonlinear Schrödinger equation must address the method of affecting time evolution and the spatial representation of the wave function and differential operators. These two topics are interrelated, and should be applied in a balanced way. Spatial representations usually consist of equally spaced grid with finite-difference approximations of differential operators [5]. Adding grid points is inefficient if high precision is needed. Instead, a global method, such as the Fourier-grid method [6], needs to be applied. A matching high-precision time evolution method must now follow.

The usual differential equation methods, such as adaptive Runge-Kutta, and Adams-Bashforth-Moulton predictor-corrector schemes (see Ref. [5] for references), as well as more recent and specialized techniques [7–9] are low order in time steps. If one is going to use a Fourier representation, as we plan to do in this paper, such a choice of temporal method yields an unbalanced overall treatment.

The widely used evolution method of Kosloff and coworkers [10–12] applicable only to the *linear* Schrödinger equation, should set the standard for nonlinear evolution. Only a global evolution approach of this kind can match the high-quality spatial representation of the Fourier grid [13]. It is the purpose of this paper to show that this can be done. The Kosloff method exploits the existence of a closed form for the evolution operator of the linear Schrödinger equation, $\psi(t)=e^{-(i/\hbar)Hit}\phi$, which is expanded by a series of Chebyshev polynomials. The resulting method is highly efficient and accurate. However, it cannot be used to treat explicitly time-dependent and nonlinear Hamiltonians.

Extension of the Kosloff method to time-dependent Hamiltonians has been made possible using a $t-t'$ formalism [14–16] or a Lanczos subspace propagation [17,18]. However, these methods are expensive because physical time is treated on an equal global footing as the space degrees of freedom and auxiliary time (t') must be introduced to affect the propagation.

In this paper, we present an evolution method which also exploits the power of the Chebyshev interpolation. However, this is done in such a way that a closed form for the evolution operator is no longer needed, so that nonlinear and explicitly time-dependent Hamiltonians can be treated. We achieve this by performing the Chebyshev interpolation *in the time domain* instead of the energy domain, as effectively done in the Kosloff method [12]. This alternative treatment is flexible enough to treat both time-dependent and nonlinear Hamiltonians. We describe the method in Sec. II, and then, in Sec. III, show several examples of its use in the context of Bose-Einstein condensation, since this admits the simplest archetype of nonlinear Schrödinger equations.

II. METHOD

The following integral equation is equivalent to the Schrödinger equation:

$$\psi(t)=\phi-\frac{i}{\hbar}\int_0^t\hat{H}(\{\psi(\tau)\},\tau)\psi(\tau)\,d\tau, \qquad (2)$$

*FAX: +972-2-6513742. Email address: roib@fh.huji.ac.il

 ©2000 The American Physical Society

where $\hat{H}=-(\hbar^2/2\mu)\nabla^2+\hat{V}+\hat{W}$. The crux of the method is to perform the time evolution within an interval $[0,T]$, on Chebyshev sampling points. In order to understand what this means and why it is important, let us briefly outline the principles of Chebyshev approximation theory.

Suppose a function $\tilde{f}(t)$, defined in the time interval $[0,T]$, is given, and we wish to construct a polynomial $\tilde{f}_N(t)$ of a given degree $N-1$, which is best in some sense over the interval $[0,T]$. For this purpose, we first transform the function to an equivalent function defined in the interval $x\in[-1,1]$. This is done by the linear mapping $x=(2t/T)-1$ and $f(x)=\tilde{f}[1/2T(1+x)]$. We now introduce the Chebyshev polynomials [19] defined as $C_n(x)=\cos n\theta$, where $x=\cos\theta$, forming a family of orthogonal polynomials over the interval:

$$\frac{2}{\pi}\int_{-1}^{1}\frac{C_n(x)C_m(x)}{\sqrt{1-x^2}}dx=\delta_{nm}(1+\delta_{n0}). \tag{3}$$

We use Chebyshev polynomials to approximate the function by a truncated expansion of N terms, forming a polynomial of degree $N-1$:

$$f(x)\approx f_N(x)=\sum_{k=0}^{N-1}F_kC_k(x). \tag{4}$$

The expansion coefficients are defined as follows:

$$F_k=\frac{2-\delta_{k0}}{\pi}\int_{-1}^{1}\frac{f(x)C_k(x)}{\sqrt{1-x^2}}dx. \tag{5}$$

Thus, within the interval,

$$\begin{aligned}\max_x|f(x)-f_N(x)|&\approx\max_x|f_{N+1}(x)-f_N(x)|\\&=|F_N|\max_x|C_N(x)|\leqslant|F_N|.\end{aligned} \tag{6}$$

The magnitude of F_N approximately bounds the truncation error of the approximation. It can be proved that this method of generating the coefficients leads to the best converging polynomial approximation in the maximum norm [19]. This result is closely related to the fact that of all N-degree polynomials $p_N(x)=x^N+a_{N-1}x^{N-1}+\cdots+a_0$, the polynomial $2^{-N}C_N(x)$ is the smallest (maximum normwise) in the interval $[-1,1]$.

We then find that this procedure for approximating functions is a ''best-fit technique.'' We now add to this fact the concept of the Gaussian quadrature, also called ''quadrature of the highest degree of algebraic precision.'' [20] This technique is applied to the integrals that define the expansion coefficients. The Gaussian quadrature theory implies that the following rank-N quadrature rule is exact for all polynomials of degree $2N-1$ [20]:

$$\int_{-1}^{1}\frac{p(x)}{\sqrt{1-x^2}}dx\approx\frac{\pi}{N}\sum_{n=0}^{N-1}p(x_n), \tag{7}$$

where the points x_n are the N roots of the Nth Chebyshev polynomial $C_N(x)$:

$$x_n=\cos\left(\frac{\pi\left(n+\frac{1}{2}\right)}{N}\right),\quad n=0,1,...,N-1. \tag{8}$$

Applying the Gaussian quadrature to the orthogonal relations of the Chebyshev polynomials [Eq. (3)] of order $n<N$ shows

$$\frac{2}{N}\sum_{k=0}^{N-1}C_n(x_k)C_m(x_k)=\delta_{nm}(1+\delta_{n0}). \tag{9}$$

Thus the following reciprocal relations concerning $f(x)$ are valid:

$$f(x)\approx\sum_{n=0}^{N-1}F_nC_n(x), \tag{10}$$

$$F_k=\frac{2-\delta_{k0}}{N}\sum_{n=0}^{N-1}f(x_n)C_k(x_n). \tag{11}$$

We already noted that the Chebyshev approximation enjoys the flavor of a best fit. Using Eq. (9), it is now evident that simultaneously it is also an *interpolation*, since it is *exact on the sampling points*:

$$f(x_n)=\sum_{k=0}^{N-1}F_kC_k(x_n). \tag{12}$$

In conclusion, the advantage of sampling a function at the roots of the Nth Chebyshev polynomial is that the resulting representation is exact at the sampling points (as with any interpolation) and, concurrently, *between the sampling points* one is assured that the truncation error is uniformly spread (best-fit flavor).

We summarize by writing the completeness and orthogonal properties of the Chebyshev polynomials on the N sampling points:

$$\sum_{n=0}^{N-1}C_k(x_n)C_{k'}(x_n)=\frac{N}{2-\delta_{k,0}}\delta_{k,k'}. \tag{13}$$

$$\sum_{k=0}^{N-1}\frac{2-\delta_{k0}}{N}C_k(x_n)C_k(x_{n'})=\delta_{n,n'}. \tag{14}$$

Once the interpolation is implemented, integrals over the interpolated function can be performed analytically:

$$\begin{aligned}\int_0^t\tilde{f}(\tau)d\tau&=\frac{T}{2}\int_{-1}^{t}f(x')dx'\\&=\frac{T}{2}\sum_{k=0}^{N-1}F_k\int_{-1}^{x}C_k(x')dx'\\&=\frac{T}{2}\sum_{k=0}^{N-1}F_kS_k(x)\end{aligned} \tag{15}$$

[note that the transformation $t=\frac{1}{2}T(1+x)$ is used]. With notation $x=\cos\theta$, it is straightforward to show that

$$S_k(\cos\theta)=\frac{\cos\theta\cos k\theta-1+k\sin k\theta\sin\theta}{k^2-1}\quad(k\neq 1), \tag{16}$$

$$S_1(\cos\theta)=\frac{\sin^2\theta}{2}. \tag{17}$$

With this Chebyshev expansion, we write any time integral directly in terms of the function values at the sampling points,

$$\int_0^t \tilde{f}(\tau)d\tau=T\sum_{n=0}^{N-1} f(x_n)I_n\left(\frac{2t}{T}-1\right), \tag{18}$$

where

$$I_n(x)=\sum_{k=0}^{N-1}\frac{2-\delta_{k0}}{2N}C_k(x_n)S_k(x). \tag{19}$$

Equations (18) and (19) are the central equations of the method. They give the integral of a function of time as a linear combination of the function values at the Chebyshev sampling points. We underline once again the reason these expressions are essential. By increasing the number of sampling points, the underlying polynomial approximation is improved, *not only* because it is accurate on more sampling points but equally important because it is more accurate *in between* them. This is not the case, for example, when equally spaced points are used.

Using Eq. (19), we now return to the numerical solution of the Schrödinger equation. The integral Schrödinger equation [Eq. (2)] now becomes an implicit equation for $\psi(t_n)$ at the sampling points

$$\psi(t_m)=\phi-\frac{iT}{\hbar}\sum_{n=0}^{N-1}\hat{H}[\psi(t_n),t_n]\psi(t_n)I_{nm}, \tag{20}$$

where, $I_{n,m}=I_n(x_m)$. This implicit equation can be solved by setting $\psi^0(t_n)=e^{-i\langle\phi|\hat{H}(\phi)|\phi\rangle t_n}\phi$, and then performing the following iteration to convergence:

$$\psi^{L+1}(t_m)=\phi-\frac{iT}{\hbar}\sum_{n=0}^{N-1}\hat{H}[\psi^L(t_n),t_n]\psi^L(t_n)I_{nm}. \tag{21}$$

Once the self-consistent solution is obtained, the entire time dependence within the interval is determined by the Chebyshev interpolation:

$$\Psi_k=\frac{2-\delta_{k0}}{N}\sum_{n=0}^{N-1}\psi(t_n)C_k\left(\frac{2t_n}{T}-1\right),$$
$$\psi(t)=\sum_{k=0}^{N-1}\Psi_k C_k\left(\frac{2t}{T}-1\right). \tag{22}$$

Algorithm

Memory. The wave function at N different times $\psi_n=\psi(t_n)$ must be stored in RAM, and $N+1$ additional wave functions Ψ_n and Θ are needed as well in RAM.

(1) Initial guess: For $n=0\ldots N-1$, $\psi_n=\phi$.
(2) Set $n'=0$. For $n=0\ldots N-1$, $\Psi_n=\phi$.
(3) $\Theta=H(\psi_{n'},t_{n'})\psi_{n'}$.
(4) For $n=0\ldots N-1$: $\Psi_n=\Psi_n-iT\times I_{n',n}\Theta$.
(5) If $(n'<N)$, $n'=n'+1$; go to (3).
(6) For $n=0$ to $N-1$, $\psi_n=\Psi_n$.
(7) Repeat from step (2), until converged self-consistent functions are achieved.
(8) Once ψ_n are at hand, use Eq. (22) to determine $\psi(t)$ for any desired $t\in[0,T]$.

At this point, we should discuss how to estimate the required number of Chebyshev sampling points in the interval. A detailed discussion appears in the Appendix.

The method works well even for relatively large intervals T. The size of the interval cannot be increased indefinitely, because the iterations start to converge slowly or even diverge altogether. A more efficient iterative process is clearly desirable; however, this issue will be addressed in future developments of the method. In this paper, we use short enough interval lengths so that convergence is efficient. As will be shown in the examples, the use of short or long intervals does not affect the extremely high accuracy achievable with this method.

The cost in memory of the method depends on the length of the interval. It is found that a reasonable small interval includes between 3 and 5 sampling points, which means that 7–11 auxiliary copies of the wave function are needed. The amount of numerical work can be measured by the number of Hamiltonian operations. This equals the number of sampling points times the number of iterations (currently, between five and ten). Thus, at present, the method is about 5–10 times more expensive than the Kosloff method (because of nonlinearity) in terms of CPU and memory requirements. While this means that the Kosloff method should be preferred for the linear Schrödinger equation, this price has to be paid for the nonlinear case, unless a substantial reduction in the number of iterations can be achieved.

III. A BOSE-EINSTEIN CONDENSATE

We chose the simplest archetype of nonlinear Schrödinger equations, the Gross-Pitaevskii theory [4] of the weakly interacting BEC. This theory yields a simple yet illuminating description of a BEC, where familiar quantum effects are distorted by nonlinear artifacts [21].

The energy functional of an interacting Bose-Einstein condensate within the Gross-Pitaevskii mean-field theory is

$$E(\psi)=\left\langle\psi\left|\frac{P^2}{2\mu}+V(r)+\frac{1}{2}A|\psi(r)|^2\right|\psi\right\rangle, \tag{23}$$

where $\psi(r)$ is the macroscopic coherent wave function, and $V(r)$ is an effective trap confining the condensate. We take the condensate wave function normalized to 1.0, while the condensate particle number, as well as the two-body interac-

tion strength (derived from the scattering length) are absorbed in the nonlinear constant A.

The Hamiltonian operator corresponding to this energy functional is obtained from the functional gradient

$$H(\psi)\psi(r)=\frac{\delta E(\psi)}{\delta\psi^*(r)}=\left[\frac{P^2}{2\mu}+V(r)+A|\psi(r)|^2\right]\psi(r). \tag{24}$$

For the purpose of demonstrating the time evolution method, here we study the ground state, the low-lying excitations, and the aperture leakage of a one-dimensional (1D) BEC.

A. 1D BEC ground state

The BEC is cooled to its ground state by evolving it in imaginary time. We start from an arbitrary state $\phi(r)$ and propagate the equation,

$$\hbar\frac{d\psi}{dt}=[\mu-H(\psi(t))]\psi(t), \quad \psi(0)=\phi, \tag{25}$$

where μ, the norm conservation Lagrange multiplier, is adjusted so as to keep the norm of ψ equal to 1 (since the exact imaginary time dynamics are not of interest, only the final result is important; this needs only be strictly required towards the last iterations). Because H is a gradient of the energy, the resulting motion leads to a steepest-descent-type method, forcing the wave function to the minimum energy $E(\psi)$. We consider a harmonic trap,

$$V(x)=\tfrac{1}{2}\mu\omega^2x^2, \tag{26}$$

where we work in units of time and distance such that $\hbar=1$, $\mu=0.5$, and $\omega=1$. We also consider an anharmonic potential, which for definiteness we take as a Morse form,

$$V(x)=V_0(1-e^{-\alpha x})^2, \tag{27}$$

and, in the same units, $V_0=6.25$ and $\alpha=0.2$. This set of parameters leads to the same second derivative at the $x=0$ well minimum as that of the harmonic potential of Eq. (26). The ground-state energies we find for the 1D BEC in these traps are shown as a function of the nonlinear constant in Fig. 1.

It is important to study the qualities of the global spatial representation, and we use the ground-state computations for this purpose. In the linear equation, the number of spatial grid points is determined by the largest potential-energy difference [11] $\Delta V=V_{\max}-V_{\min}$. For the nonlinear case, this type of analysis cannot be valid in general. When the nonlinearity constant is positive, however, a simple extension can be formulated with ΔV increased by a small multiple of the nonlinear potential. However, when A is negative, extremely high-kinetic-energy components are important for stabilizing the 1D BEC against collapse, and a high spatial frequency representation is required. The convergence of the ground-state energy with respect to the spatial grid spacing can be studied in Fig. 2. As the nonlinearity constant grows in magnitude, the grid spacing required for achieving a given relative error grows. However, when A is negative, the required grid spacing is much smaller.

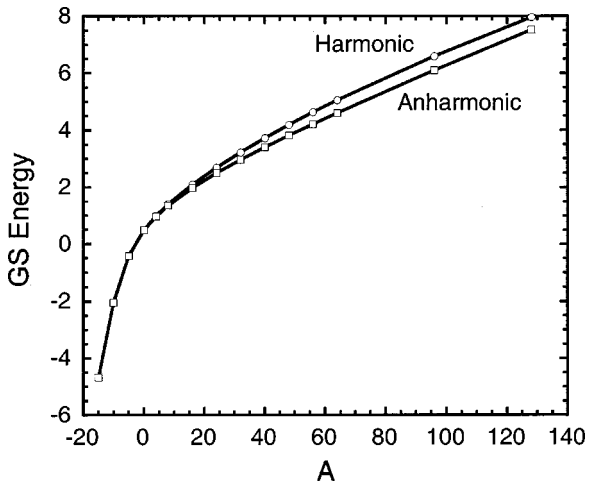

FIG. 1. The ground-state energy of a BEC for harmonic and anharmonic potentials.

B. Low-lying dipole excitations of BEC

The method of computing low-lying excitation in the BEC consists of perturbing the ground-state wave function $\psi_{\rm gs}$, and then measuring the time dependent response. Here we follow Ref. [7], and apply a small momentum kick $p=\hbar k$:

$$\psi_k(x)=e^{-ikx}\psi_{\rm gs}.$$

The response is determined by time evolution according to the real-time Schrödinger equation:

$$i\hbar\frac{d\psi}{dt}=H(\psi(t))\psi(t), \quad \psi(0)=\psi_k.$$

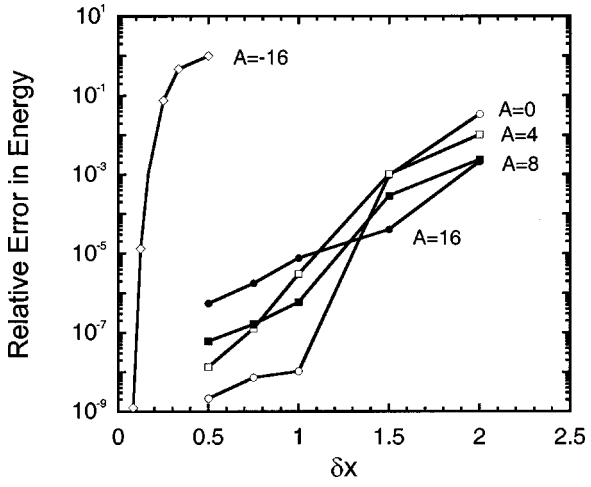

FIG. 2. Convergence of the ground-state energy of a BEC with grid spacing. Shown are the relative discretization errors in the Fourier spatial representation for several values of the nonlinearity constant.

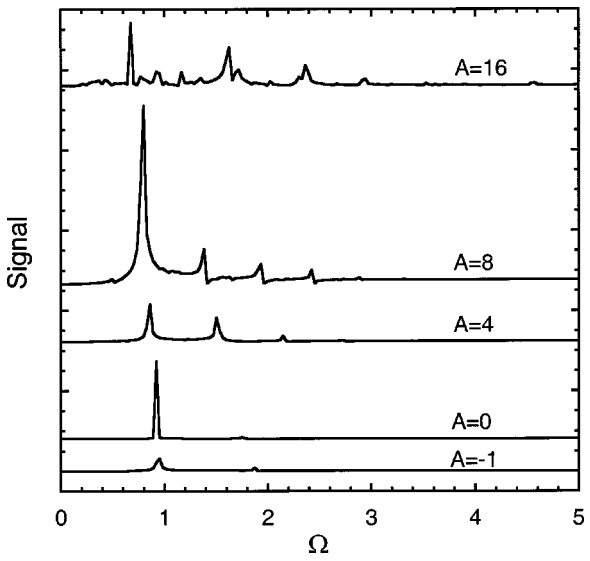

FIG. 3. The ground-state excitation spectrum of a BEC in an anharmonic trap for various values of the nonlinear constant. It is seen that the spectrum shifts and new lines are formed as this constant is varied.

During this evolution in time, the position signal $r(t) = \langle \psi(t)|\hat{r}|\psi(t)\rangle$ executes an intricate oscillatory motion, involving frequencies related to excitation energies of the BEC, which can be resolved by a Fourier analysis.

We first apply this method to a BEC in a harmonic trap [Eq. (26)]. We found that the condensate exhibits only a single excitation energy, with the same frequency as a harmonic oscillator, $\omega = 1$. This was confirmed up to a large nonlinear constant $0 \leqslant A \leqslant 128$. Thus, in the ground state of a harmonic trap, the BEC ground-state dipole excitations are identical to that of a simple harmonic oscillator.

Next, an anharmonic trap was examined [Eq. (27)]. The computation was performed using a spatial grid extending from $x_0 = -6$, to $x_f = 10$, with a grid spacing $\delta x = 1$. The frequency resolved spectra for several values of A are shown in Fig. 3, and the strong influence of the condensate nonlinearity on the ground-state excitation spectrum is observed.

In order to appreciate the magnitude of the numerical errors incurred by evolution, we performed three computations of the time dependent trajectory $r(t) = \langle \psi(t)|\hat{r}|\psi(t)\rangle$ of the anharmonic oscillator, with $A = 8$. All three trajectories start from the same initial kicked ground state, and are computed using 2000 time steps of size $T = 0.1$, totaling to time $T_f = 200$. Each trajectory was computed using a different number N of sampling points of the T interval (with $N = 5$, 10, and 20 points used, respectively). The time propagation error incurred in the first two trajectories can be estimated by the quantities $e_n(t) = r_n(t) - r_3(t)$ ($n = 1$ and 2). The rate of error accumulation $e_n(t)/t$ is plotted in Fig. 4. It is can be inferred that the time propagation error is readily eliminated by increasing the number of sampling points N. Furthermore, the error grows only linearly with time.

C. Aperture leakage

When a hole is made in the confining potentials of a BEC, the gas can flow out. We affect such an aperture by coupling

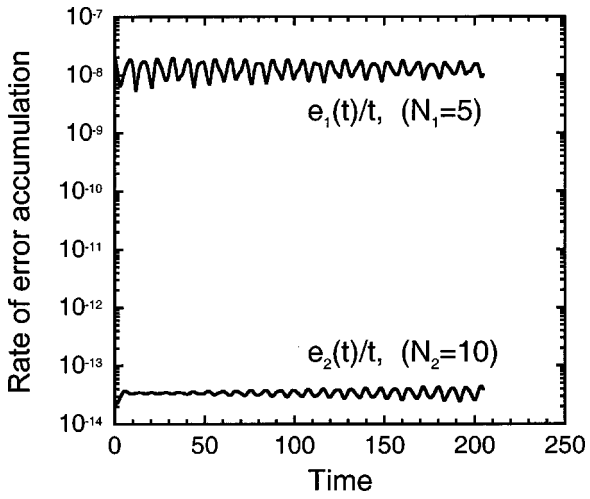

FIG. 4. Time-propagation error accumulation. Shown is the rate of numerical error accumulation, computed as discussed in the text. The constant error accumulation rate is evident as is the drastic reduction of the error by doubling the number of sampling points. The time step is $T = 0.1$.

to a repulsive potential. Suppose the confining potential is $V(x)$, and the repulsive potential is an exponential potential $V_{\rm ex}(x) = Ke^{-\beta(x-x_e)}$ ($K > 0$); then the coupling of the two takes the following form (see Fig. 5):

$$V_A(x) = \frac{V(x) + V_{\rm ex}(x)}{2} \left[\left(\frac{V(x) - V_{\rm ex}(x)}{2} \right)^2 + C^2 \right]^{1/2}. \tag{28}$$

The parameters for this numerical experiment are shown in Table I.

A negative imaginary potential is placed at the positive grid boundary to absorb the outgoing BEC flux. This well-studied technique prevents spurious edge effects such as reflection or wraparound [22]. The resulting potential exhibits a high potential barrier, so leakage through this barrier is small. The time-dependent leaking wave packets for $A = 0$ and 4 are shown in Figs. 6 and 7. Due to the self-repulsion,

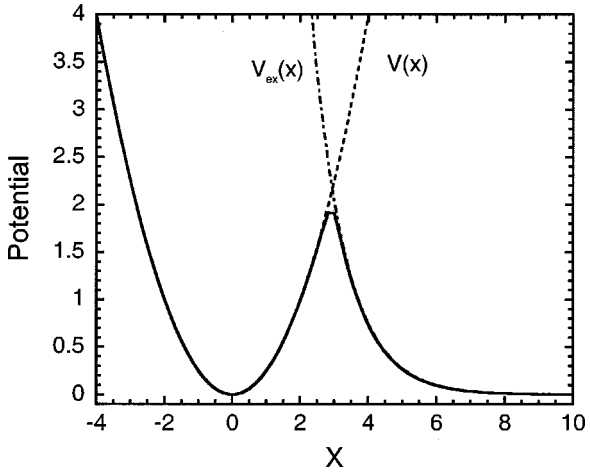

FIG. 5. An aperture in the confining potential of the BEC, enabling tunneling.

TABLE I. Parameters of the aperture.

Parameter	Value
K	15
x_0	1
γ	1
C	0.2

the condensate finds it easier to leak through the aperture as the positive nonlinear constant becomes larger.

IV. SUMMARY

We have presented a highly accurate and efficient method for propagating the nonlinear time-dependent Schrödinger equation. The method combines an implicit approach with Chebyshev interpolation in the time domain. In combination with a Fourier or plane-wave spatial representation it leads to an overall balanced numerical method. Although we have shown only examples where the spatial part is one dimensional, the method is straightforwardly applicable to more spatial dimensions, since there is no direct dependence of the time evolution and sampling points on the spatial grid. Indeed, the present method was recently implemented for electronic structure [23], using a time-dependent formalism, and accurate time evolution was achieved with no difficulty.

ACKNOWLEDGMENTS

I would like to express my gratitude to R. Kosloff for his valuable comments and suggestions regarding this work. This research was supported by Grant No. 9800108 from the United States–Israel Binational Science Foundation (BSF), Jerusalem, Israel. I also thank Santiago Alvarez from the University of Barcelona where most of this work was conceived.

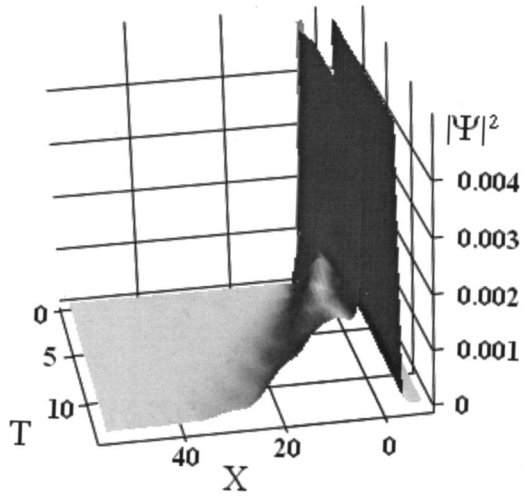

FIG. 6. Tunnel leakage of a BEC with no interactions ($A=0$). At a time $T=0$ a hole is made in the confining potential [see Eq. (28)]. As a result, a small tunneling current forms, and the condensate leaks out.

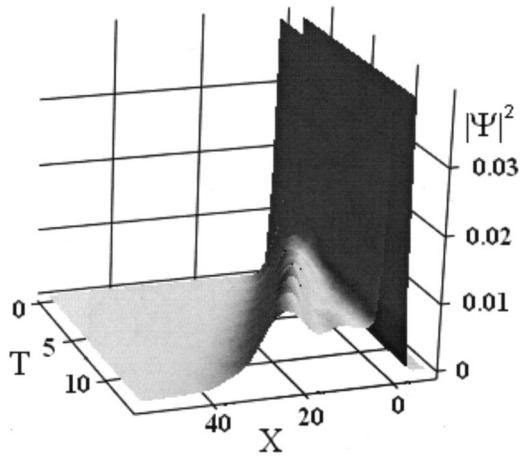

FIG. 7. Same as Fig. 6, with $A=4$. The tunneling rate is enhanced by the interparticle repulsion.

APPENDIX: DETERMINING THE REQUIRED NUMBER OF CHEBYSHEV SAMPLING POINTS

Let us determine the number of Chebyshev sampling points required for representing a high-frequency component Ω. This can be done by inspecting the Chebyshev coefficients of $\tilde{f}(t)=e^{i\Omega t}$:

$$F_k=\frac{2}{\pi}e^{i(1/2)\Omega T}\int_{-1}^{t}\frac{e^{i(1/2)\Omega Tx}C_k(x)}{\sqrt{1-x^2}}dx$$

$$=2i^k e^{i(1/2)\Omega T}J_k\left(\frac{1}{2}\Omega T\right). \tag{A1}$$

The asymptotic properties of Bessel functions are well known [24], and it is established that, for large values of k,

$$J_k\left(\frac{1}{2}\Omega T\right)-\frac{1}{\sqrt{2\pi k}}\left(\frac{e\Omega T}{4k}\right)^4 \tag{A2}$$

Thus, once $k>(e/4)\Omega T$, the coefficients drop off exponentially fast, becoming zero to machine accuracy after a small number of additional terms N_r. Thus the number of sampling points is

TABLE II. Values of N_r leading to maximum norm precisions of 10^{-4} and 10^{-8} in the Chebyshev approximation of $f(x)=e^{i(1/2)\Omega Tx}$.

$\frac{1}{2}\Omega T$	N_r (units of 10^{-4})	N_r (units of 10^{-8})
1	5	8
2	5	9
4	6	11
8	6	12
16	6	13
32	6	14
64	6	15
128	6	15
256	6	15

$$N = \frac{e}{4}\Omega T + N_r \tag{A3}$$

where N_r is given in Table II.

It is now important to estimate the maximal frequency in the system. Also, it is important to arrange the Hamiltonian in a balanced way so as to minimize the maximal frequency, for example, for a time-independent linear Hermitian Hamiltonian with maximal eigenvalues $E_{\max}$ and minimal eigenvalues $E_{\min}$ one can shift the Hamiltonian: $H_{\text{shifted}} = H - [(E_{\max} + E_{\min})/2]$, making the largest frequency equal to $\Omega = (E_{\max} - E_{\min})/2$. For a nonlinear Hamiltonian, it is more intricate to estimate what the highest frequencies are, however, it is our experience that the nonlinearity does not build temporal frequencies beyond the ones taken into account by the consideration above.

[1] W. Negele, Rev. Mod. Phys. **54**, 913 (1986).
[2] R. B. Gerber and M. A. Ratner, Adv. Chem. Phys. **70**, 97 (1988).
[3] E. Runge and E. K. U. Gross, Phys. Rev. Lett. **52**, 997 (1984).
[4] P. Nozieres and D. Pines, *The Theory of Quantum Liquids*, Vol. II (Addison-Wesley, Redwood City, CA, 1990).
[5] W. H. Press, S. A. Teukolsky, W. T. Vetterling, and B. P. Flannery, Numerical Recipes in C, 2nd ed. (Cambridge University Press, Cambridge, 1992).
[6] D. Kosloff and R. Kosloff, J. Comput. Phys. **52**, 35 (1983).
[7] K. Yabana and G. F. Bertsch, Phys. Rev. B **43**, 4484 (1996).
[8] M. D. Feit, J. A. Fleck, and A. Steiger, J. Comput. Phys. **47**, 412 (1982).
[9] H. Jiang and X. S. Zhao, Chem. Phys. Lett. **319**, 555 (2000).
[10] H. Tal-Ezer and R. Kosloff, J. Chem. Phys. **81**, 3967 (1984).
[11] R. Kosloff, J. Phys. Chem. **92**, 2087 (1988).
[12] R. Kosloff, Annu. Rev. Phys. Chem. **45**, 145 (1994).
[13] C. Leforestier, R. H. Bisseling, C. Cerjan, M. D. Feit, R. Friesner, A. Guldberg, A. Hammerich, G. Jolicard, W. Karlein, H.-D. Meyer, N. Lipkin, O. Roncero, and R. Kosloff, J. Comput. Phys. **94**, 59 (1991).
[14] P. Pfeifer and R. D. Levine, J. Chem. Phys. **79**, 5512 (1983).
[15] U. Peskin, R. Kosloff, and N. Moiseyev, J. Chem. Phys. **100**, 8849 (1994).
[16] G. Yao and R. E. Wyatt, J. Chem. Phys. **101**, 1904 (1994).
[17] G. Yao and R. E. Wyatt, Chem. Phys. Lett. **239**, 207 (1995).
[18] C. S. Guiang and R. E. Wyatt, Int. J. Quantum Chem. **67**, 273 (1998).
[19] T. J. Rivlin, *Chebyshev Polynomials: From Approximation Theory to Algebra and Numbers Theory* (Wiley, New York, 1990).
[20] V. I. Krylov, *Approximate Calculation of Integrals*, translated by A. H. Stroud (Macmillan, New York, 1962).
[21] P. A. Ruprecht, M. J. Holland, K. Burnett, and M. Edwards, Phys. Rev. A **51**, 4704 (1995).
[22] D. Neuhauser and M. Baer, J. Chem. Phys. **90**, 4351 (1989).
[23] R. Baer (unpublished).
[24] *Handbook of Mathematical Functions*, edited by N. Abramowitz and I. A. Stegan (Dover, New York, 1972).